EXPERIMENTAL AND ANALYTICAL INVESTIGATION OF THE STATIC STRENGTH OF INVOLUTE SPLINE CONNECTIONS

Muhammet Furkan NADAROĞLU[1]/ Dr. Öğr. Üyesi Murat ŞEN[2]/ Doç. Dr. Selim HARTOMACIOĞLU[3]
[1]TAAC HAVACILIK TEKNOLOJİLERİ, furkan.nadaroglu@taac.com.tr,
ORCID: 0009-0006-8965-6373
[2]Marmara University, Technology Faculty, Mechanical Engineering, murat.sen@marmara.edu.tr,
ORCID: 0000-0003-2216-245X
[3] Marmara Üniversitesi, Teknoloji Fakültesi, Makine Mühendisliği, selimh@marmara.edu.tr
ORCID: 0000-0002-4541-4894

Abstract

Involute spline connections play a critical role in machine element design due to their high torque transmission capacity and ability to provide precise angular alignment. The design and selection of such connections are defined within the framework of international standards such as DIN 5480 and, in particular, ANSI B92.1, which is adopted in this study. This research investigates the static strength behavior of involute spline connections defined according to the ANSI B92.1 standard using a systematic experimental design approach based on the Taguchi L8 orthogonal array. Within the experimental design, the combined effects of three fundamental geometric parameters at two levels each were evaluated. These parameters were identified as contact face width (10 mm and 20 mm), spline root type (flat and fillet), and the diametral pitch–number of teeth combination (16/32” DP – 8 teeth and 32/64” DP – 16 teeth). The static strength of each spline configuration was estimated through numerical analyses based on the Niemann/Winter analytical approach using KISSsoft engineering software. In addition to the numerical analyses, destructive static torsion tests under increasing torque were conducted on spline specimens manufactured from Ck 45 steel. Manufacturing tolerances and experimental conditions were kept constant throughout all tests to ensure the comparability of the results. For each experimental configuration, the primary output parameters were defined as KISSsoft-based analytical static strength values, experimentally measured fracture torques, and the associated manufacturing costs. The experimental findings revealed that, for all specimens, failure occurred in the form of torsional fracture of the spline cross-section prior to any tooth contact or tooth root damage. Post-test examinations indicated no significant damage on the spline teeth, demonstrating that the failure mechanism was governed by the torsional load-carrying capacity of the spline cross-section rather than the tooth load capacity. This result emphasizes that, in static strength evaluations of spline connections, not only the tooth load capacity but also the torsional strength of the spline cross-section must be taken into account. Overall, this study aims to identify the optimum involute spline configuration in terms of both strength and manufacturability by integrating analytical predictions, experimental results, and manufacturing-related considerations.

Key Words: Involute spline, static torsional strength, Niemann/Winter method, optimization

1. INTRODUCTION

Involute spline connections are a crucial mechanical interface in modern power transmission systems, where high torque capacity, precise alignment, and reliable load transfer are essential design requirements (Niemann & Winter, 2003; Budynas & Nisbett, 2020). These components are widely used in demanding environments, including automotive drivelines, heavy machinery gear trains, aerospace actuators, and various industrial motion-control assemblies. The primary advantage of involute splines lies in their tooth profile, which allows for superior load distribution across multiple teeth and facilitates self-centering, inherently minimizing misalignment stresses compared to simpler key or bolt connections.

However, despite their widespread use, the performance of involute splines is governed by a complex interplay of geometric, material, and assembly-related factors. Design decisions such as contact surface length, specific root profile type (flat vs. fillet), and the selection of Diametral pitch (DP) & tooth count and collectively influence load distribution, stress concentration at critical locations, overall manufacturability, and assembly consistency (Budynas & Nisbett, 2020; Michałowski & Gaska, 2018). When these combined parameters are not optimally configured, the system can suffer from significant issues, including premature wear, fretting corrosion, unacceptable noise levels, and even catastrophic torque-transfer failure due to excessive root stress or shear. Consequently, the need for a systematic, quantitatively supported method to optimize spline geometry has become increasingly evident.

The geometry and tolerances of involute splines are standardized by internationally recognized specifications to ensure interchangeability and predictable performance. Two prominent standards are the DIN 5480 (German Institute for Standardization), which is widely used in Europe, and the ANSI B92.1 (American National Standards Institute), which is predominant in North American and many other global markets (ANSI, 2011; DIN, 2011; AGMA, 2018). Both standards provide detailed specifications for tooth profiles, fits, and tolerances, but the specific choice of geometric parameters within these standards (e.g., fit class, root geometry, and length) remains a critical factor for achieving optimal performance in a specific application.

The present study addresses the gap in integrated analysis by evaluating the combined effects of the critical parameters—contact surface width, root type, and Diametral pitch (DP) & tooth count configuration—using geometries strictly defined by ANSI B92.1 (ANSI, 2011) and supported by AGMA design guidelines (AGMA, 2018). Utilizing KISSsoft-based numerical analyses and the Taguchi L8 orthogonal design, the research aims to identify the dominant factors influencing static strength and to determine an optimal design setting that balances structural integrity with manufacturing feasibility. The main contribution of this study lies in experimentally demonstrating that, under static torsional loading, the failure of involute spline connections can be governed by cross-sectional torsional strength rather than tooth contact stress, and in critically assessing the applicability of the Niemann/Winter method under such conditions.

2. MATERIALS AND METHODS

2.1 Material

The material selection and environmental conditions were defined identically for both the experimental tests and the numerical analyses in order to ensure direct comparability between analytical predictions and experimental results. By keeping the material properties and testing environment constant throughout the study, the influence of geometric design parameters on the static strength of involute spline connections could be isolated and evaluated objectively.

All external involute spline specimens investigated in this study were manufactured from Ck 45 medium-carbon steel, which is widely used in industrial power transmission applications due to its balanced combination of

strength, machinability, and cost-effectiveness. No heat treatment, surface hardening, or post-processing operations were applied to the external spline specimens. This deliberate choice was made to eliminate the influence of material strengthening mechanisms and to ensure that the observed failure behavior was governed primarily by the base material properties and spline geometry rather than by surface-related effects.

The internal spline component used in the experimental test setup was manufactured from AISI 4340 alloy steel. Compared to Ck 45, AISI 4340 exhibits significantly higher strength and toughness, allowing the internal spline to remain elastic and undamaged during all experimental runs. This configuration ensured that failure consistently occurred in the external spline specimens, enabling multiple tests to be conducted using the same internal spline adaptor while maintaining experimental repeatability and consistency.

For the numerical analyses performed using KISSsoft software, the material properties of Ck 45 and AISI 4340 were defined in accordance with standard material databases embedded within the software environment. The same material definitions were applied consistently across all analytical models to maintain one-to-one correspondence with the experimentally tested specimens.

All experimental tests and numerical analyses were conducted under controlled laboratory conditions at standard room temperature. Environmental factors such as ambient temperature and humidity were kept constant throughout the study, and their potential influence on material behavior was considered negligible. Consequently, both experimental and analytical evaluations were performed under equivalent environmental conditions, ensuring that the observed differences in static strength could be attributed solely to the investigated geometric parameters.

2.2 Method

This study adopts the Taguchi L8 Orthogonal Array to efficiently investigate the influence of three primary design factors (A, B, C) at two distinct levels (L1, L2) (Taguchi, 1986; Ross, 1996). The L8 array, which is a fractional factorial design, allows for the independent assessment of the main effects of these three factors with only eight experimental runs (Yadav & Pathak, 2020).

The control factors and their assigned levels are as follows:

Table 1. Control factors and levels

Factor	Description	Level 1 (L1)	Level 2 (L2)
A	Contact Surface Width	10 mm	20 mm
B	Spline Root Type	Flat Root Side Fit	Fillet Root Side Fit
C	Diametral pitch (DP) & tooth count	16/32" DP 8T 30° PA	32/64" DP 16T 30° PA

Following the definition of the control factors and their corresponding levels in Table 1, each factor is further explained using representative spline geometries in order to clarify its physical meaning and its influence on the load-carrying behavior of involute spline connections. The selected geometries are fully compliant with the ANSI B92.1 standard and are representative of the spline configurations investigated in this study.

Factor A: Contact Surface Width

Factor A represents the axial contact surface width of the spline connection, which directly influences the effective load transfer area between the mating spline teeth. Increasing the contact surface width generally enhances the load-sharing capability of the spline by distributing the transmitted torque over a larger contact area, thereby reducing local contact stresses under static loading conditions.

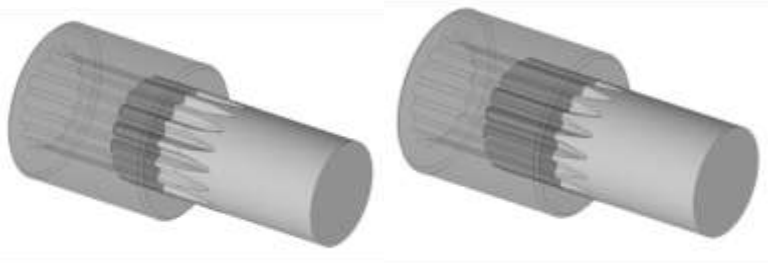

Figure 1. Spline contact width example.

Figure 1 illustrates spline configurations with higher and lower contact surface widths. As shown, a larger contact width provides a longer axial engagement length between the internal and external spline teeth, which is expected to improve static load-carrying capacity and stiffness. In the present study, two contact surface widths 10 mm and 20 mm were selected to evaluate the effect of axial engagement length on static strength.

Factor B: Spline Root Type

Factor B corresponds to the spline root geometry, which plays a critical role in stress concentration at the tooth root and influences stiffness, manufacturability, and sensitivity to misalignment. Two standardized root configurations defined by ANSI B92.1 were considered: flat root side fit and fillet root side fit.

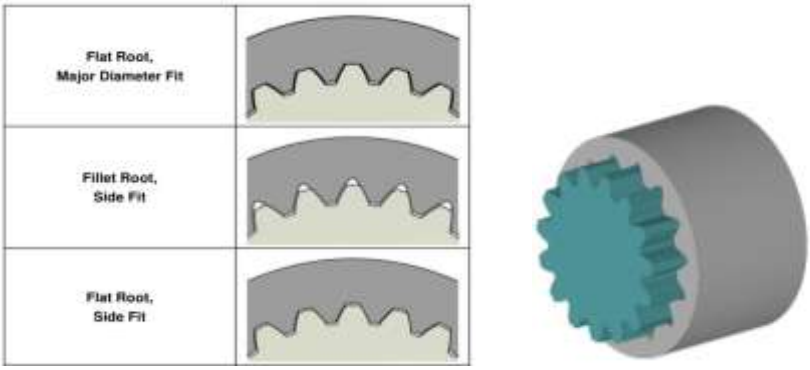

Figure 2. Spline root types / Spline pair model.

As illustrated in Figure 2, flat root side fit splines are characterized by a straight root profile, which typically results in greater tooth root thickness and higher resistance to shear under static loading. In contrast, fillet root side fit splines incorporate a curved root geometry, providing a larger root radius that reduces stress concentration and is generally associated with improved fatigue performance. Although fillet root geometries are primarily associated with fatigue-critical applications, both root types were evaluated in this study to assess their influence on static strength behavior under monotonic torsional loading (Michałowski & Gaska, 2018; Budynas & Nisbett, 2020).

Factor C: Diametral Pitch (DP) and Tooth Count

Factor C represents the combined effect of diametral pitch and number of teeth, which together define the spline tooth size, thickness, and stiffness. Two DP–tooth count combinations were selected while maintaining the same pressure angle (30°): 16/32″ DP with 8 teeth and 32/64″ DP with 16 teeth.



Figure 3. 32/64" DP 16T 30° PA and 16/32" DP 8T 30° PA spline geometries.

Figure 3 presents representative spline geometries corresponding to the two selected configurations. The lower tooth count configuration results in thicker individual teeth and increased local stiffness, whereas the higher tooth count configuration provides finer teeth with potentially improved load distribution. These configurations were chosen to investigate how tooth thickness and stiffness affect the static torque capacity of involute spline connections when evaluated under identical material and manufacturing conditions.

Based on the defined control factors and levels, a Taguchi L8 orthogonal array was constructed to determine the experimental combinations used in this study. The L8 matrix assigns each factor level systematically across eight experimental runs, ensuring balanced representation and independent evaluation of the main effects of Factors A, B, and C.

Table 2. L8 experimental matrix.

Experiment Number	A(Width)	B (Root Type)	C(Diametral pitch (DP) & tooth count)
1	10 mm	Flat Root Side Fit	16/32" DP 8T 30° PA
2	10 mm	Flat Root Side Fit	32/64" DP 16T 30° PA
3	10 mm	Fillet Root Side Fit	16/32" DP 8T 30° PA
4	10 mm	Fillet Root Side Fit	32/64" DP 16T 30° PA
5	20 mm	Flat Root Side Fit	16/32" DP 8T 30° PA
6	20 mm	Flat Root Side Fit	32/64" DP 16T 30° PA
7	20 mm	Fillet Root Side Fit	16/32" DP 8T 30° PA
8	20 mm	Fillet Root Side Fit	32/64" DP 16T 30° PA

Each row of the L8 orthogonal array corresponds to a unique spline configuration, which served as the basis for specimen manufacturing, numerical analysis, experimental testing, and production cost evaluation. This unified experimental matrix ensures consistency across all evaluation domains and allows the results to be directly compared within a single integrated framework, as discussed in the results and discussion section. Only the main effects of the control factors were considered, while higher-order interaction effects were neglected, as the objective was to identify the dominant parameters governing static strength under monotonic loading conditions.



Figure 4. Manufacturing of external involute spline specimen from Ck 45 steel.

Figure 4 shows an external involute spline specimen manufactured within the scope of this study during the spline cutting operation. The illustrated specimen is representative of all external spline specimens produced for the Taguchi L8 experimental matrix, as the same machining method and process parameters were applied to all configurations.



Figure 5. Manufactured external spline specimens (Taguchi L8 configurations).

Figure 5 shows the external involute spline specimens manufactured according to the Taguchi L8 orthogonal array configurations. Each specimen corresponds to a unique combination of the control factors defined in the experimental design. Although the spline geometries differ in terms of contact surface width, root type, and diametral pitch–tooth count combination, all specimens were produced using the same machining method, tooling, and process parameters. This ensures that geometric design variables constitute the only source of variation among the tested specimens.



Figure 6. Internal spline specimens corresponding to test configurations.

Figure 6 presents the internal spline specimens used in the experimental torsion tests. These components were manufactured to match the corresponding external spline geometries and were employed consistently across the test configurations. The internal spline specimens serve as mating components in the test assembly, enabling aligned torque transmission during experimental evaluation.

Table 3. Spline production costs by feature.

Factor	Level	Description	Unit Cost(€/piece)
A – Contact Surface (mm)	A1	10 mm	45
	A2	20 mm	70
B – Spline Type	B1	Flat Root Side Fit	35
	B2	Fillet Root Side Fit	55
C – Diametral pitch (DP) & tooth count	C1	16/32" DP 8T 30° PA	50
	C2	32/64" DP 16T 30° PA	75

Table 3 presents the factors affecting the production costs of the spline specimens tested within the L8 orthogonal array by summarizing the selected factor levels, their corresponding geometric definitions, and the associated unit production costs, which were subsequently used to determine the production cost of each individual spline specimen defined in the Taguchi L8 experimental matrix.

2.3 Static Strength Evaluation Framework

This section outlines the theoretical and experimental evaluation framework adopted to investigate the static strength behavior of involute spline connections designed within the Taguchi L8 orthogonal array. In accordance with the material definitions and manufacturing methods described in Sections 2.1 and 2.2, all spline configurations were evaluated using a consistent and unified approach to ensure comparability of the results. The static strength assessment was carried out through a combination of numerical analyses and experimental torsion tests, both applied under identical loading and boundary conditions. The detailed methodologies and assumptions associated with the numerical analysis and experimental testing procedures are presented in the following subsections.

Table 4. Evaluation criteria and engineering significance.

Evaluation Criterion	Description	Engineering Significance
Static Strength	Indicates the resistance of spline teeth to deformation or fracture under maximum load.	Reliability, torque transmission capacity
Production	Related to machining precision, tolerance class, and manufacturing time.	Overall production cost, standardization

Table 4 summarizes the evaluation criteria adopted in this study and their corresponding engineering significance. These criteria define the primary output parameters used to assess the performance of the involute spline configurations investigated within the Taguchi L8 framework. Accordingly, the static strength criterion is quantified through both numerical analysis and experimental testing, while the production criterion is evaluated based on manufacturing-related considerations. The outputs associated with these criteria constitute the basis for the comparative assessment of different spline configurations, and the results obtained from numerical analyses and experimental tests are directly compared and discussed in the subsequent sections.

2.3.1 Analytical static strength prediction (KISSsoft)

Numerical analyses were performed using KISSsoft, a dedicated software solution for machine element design, to simulate the static strength and predict the yield torque for each L8 configuration. The numerical evaluation of spline strength was performed using the Niemann/Winter analytical framework implemented in KISSsoft (Niemann & Winter, 2003). This method evaluates the load-carrying capacity of spline connections based on idealized load sharing assumptions, geometric characteristics, and material strength limits. In this study, the numerical results are interpreted as analytical estimates rather than direct failure predictions, and are compared with experimental results to identify the governing failure mechanism.

Failure Criterion: Rather than assuming a predefined failure mode, the governing failure criterion was identified by comparing the predicted torque levels associated with different limiting mechanisms (tooth contact, tooth root, and shaft torsion) with experimental observations. This approach allows the dominant failure mode to be determined based on physical evidence rather than analytical assumptions.

Figure 7 presents the input parameters defined in the KISSsoft software for the numerical analysis of Experimental Run No. 1 within the Taguchi L8 orthogonal array. The parameters highlighted in the figure indicate the selected spline standard, spline root type, number of teeth, diametral pitch (DP), tolerance class, and face width used in the numerical model. In addition, the material properties assigned to the shaft and hub components were consistently defined in accordance with the material specifications described in Section 2.1. The purpose of including this figure is to demonstrate that the numerical model established in KISSsoft is fully consistent with the geometric and material definitions of the experimentally tested spline specimens, ensuring a direct correspondence between the analytical configurations and the physical test components.

Figure 8 illustrates the numerical analysis results obtained using the input parameters defined in Figure 7, where the spline strength evaluation was performed using the Niemann/Winter analytical approach implemented in the KISSsoft software for static strength assessment of involute spline connections. As shown in the figure, the application factor (Ka) was set to 1.0 in order to ensure that the predicted failure torque obtained from the numerical analysis closely corresponds to the experimentally measured failure torque, rather than representing a design value with an intentionally high safety margin. Although the loading type is defined within the software framework, the present evaluation focuses on static strength limits rather than fatigue-related effects. In the results section, particular attention is given to the contact stress safety factor. The analysis indicates that failure is expected to occur at the torque level corresponding to a contact stress safety factor of unity for the external spline (shaft). Accordingly, the torque associated with this condition is considered the static yield (failure) torque of the spline connection for the evaluated configuration.

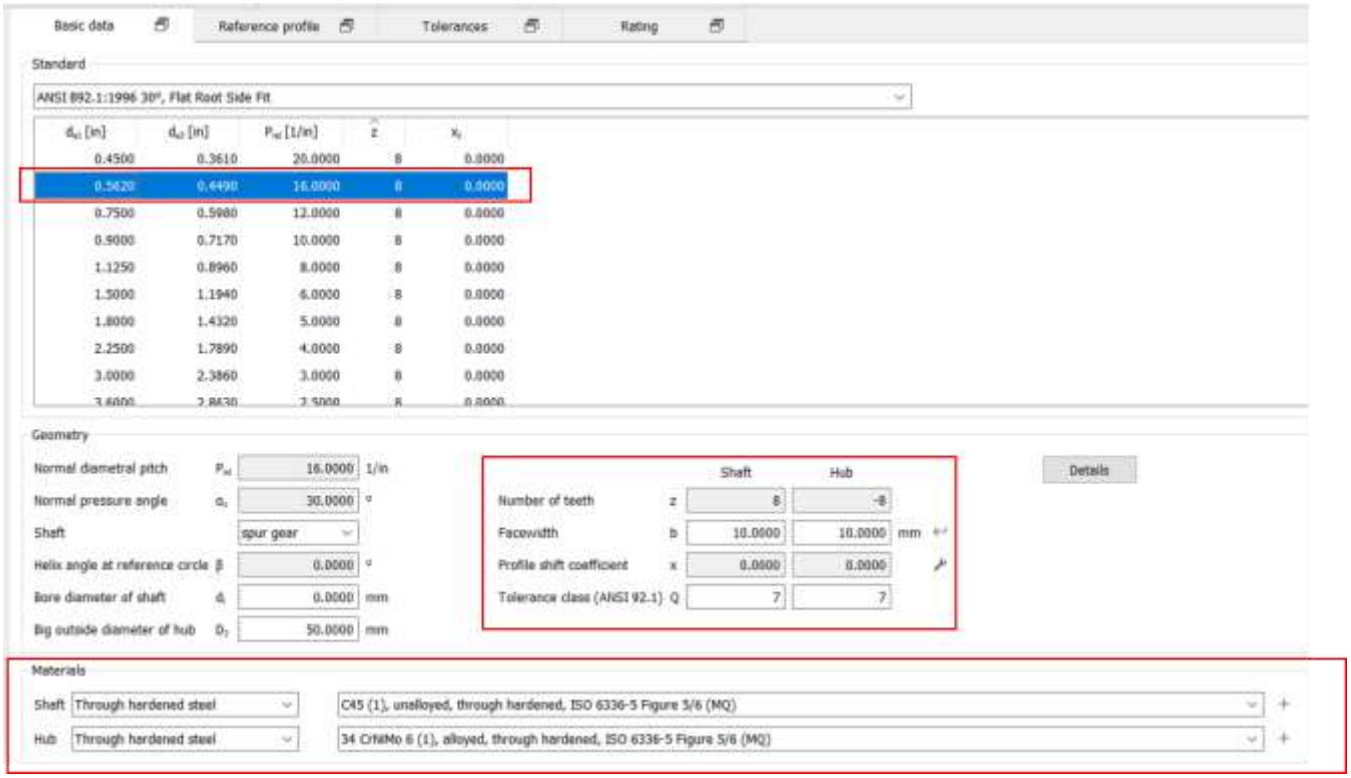

Figure 7. KISSsoft input parameters used for the numerical analysis of experimental run no. 1.

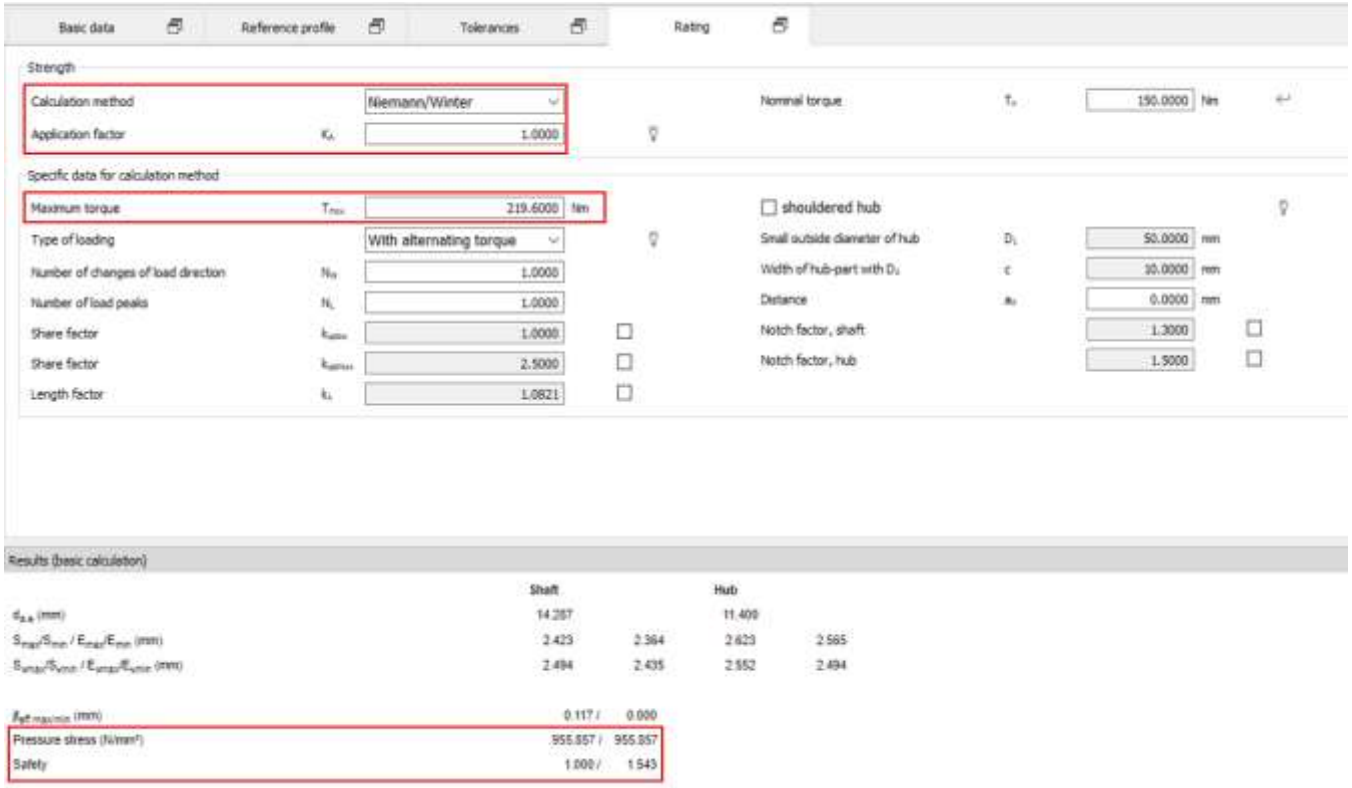

Figure 8. KISSsoft static strength analysis results for experimental run no. 1.

2.3.2 Experimental static strength prediction (Test)

In order to experimentally assess the static strength behavior of the involute spline connections, a controlled torsional testing procedure was implemented. The experimental evaluation was designed to provide a direct measurement of the static yield torque for each spline configuration defined within the Taguchi L8 orthogonal array, under well-defined and repeatable loading conditions (Gupta & Kundu, 2019; Kumar & Singh, 2021). All tests were conducted in accordance with the common material definitions and manufacturing procedures described in the previous sections, ensuring consistency between numerical analyses and experimental investigations. The experimental methodology consists of a custom-designed torsional test rig and a standardized test execution procedure, which are described in detail in the following subsections. Similar static torsion test configurations for shaft–hub connections have been reported in the literature (Kumar & Singh, 2021).

2.3.3 Test rig and assembly configuration

A custom-designed torsional test rig was developed to apply controlled static torsional loading to the involute spline specimens under well-defined boundary conditions. The test rig consists of a rigid fixture body, an internal spline adaptor, an external involute spline specimen, and a torque application mechanism. The internal spline adaptor is rigidly fixed to the fixture in order to prevent unintended rotation during loading, thereby ensuring that the applied torque is transmitted exclusively through the spline interface.

The external involute spline specimen is concentrically engaged with the internal spline adaptor and connected to the torque wrench through a dedicated coupling element. This configuration maintains axial and angular alignment between the mating spline components and minimizes parasitic bending or axial loads. The entire assembly is securely mounted on a rigid base plate, providing sufficient stiffness to prevent fixture deformation during testing and ensuring repeatable boundary conditions for all experimental runs.

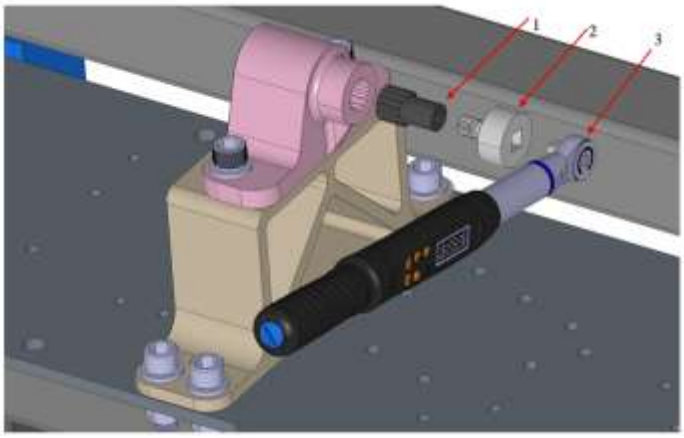

Figure 9. Exploded view of the test assembly showing the individual components.

Experimental torsion test setup showing (1) the internal involute spline (hub), (2) the external spline test specimen (shaft), and (3) the digital torque wrench used to apply and measure monotonic torsional loading until failure.

Static torsion tests were conducted to determine the experimental static yield torque of each spline configuration defined within the Taguchi L8 orthogonal array. Torque was applied manually using a calibrated digital torque wrench operating in peak-hold mode, allowing accurate recording of the maximum applied torque during each

test. The applied torque was increased incrementally at a controlled rate, thereby maintaining quasi-static loading conditions.

Each test was continued until a clear and irreversible failure of the external spline specimen was observed. The peak torque recorded at the onset of failure was defined as the experimental static yield torque for the corresponding spline configuration. After each test, the internal spline adaptor and the test fixture were inspected to confirm the absence of damage, enabling consistent reuse across multiple experimental runs. This procedure ensured both the repeatability and comparability of the experimental results across all spline configurations.

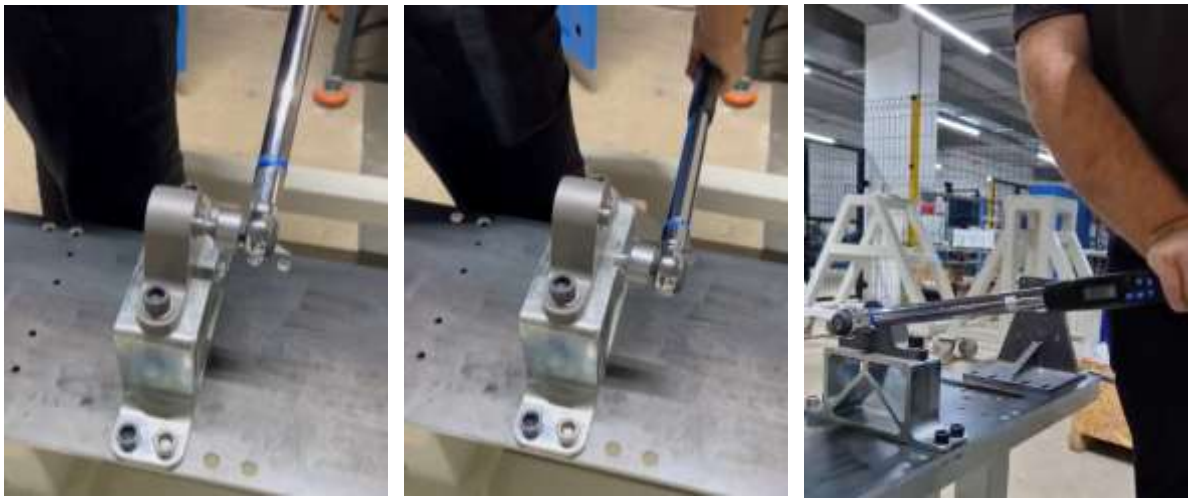

Figure 10. Assembled test rig under aligned loading conditions.



Figure 11. Experimental failure mode of the external spline specimen under static torsional loading.

3. RESULT AND DISCUSSION

This section presents the experimental and analytical findings obtained for the involute spline configurations defined within the Taguchi L8 orthogonal array. Based on the common material definitions, manufacturing procedures, numerical analysis framework, and experimental testing methodology described in the previous sections, the key output parameters were determined for each experimental run. The results corresponding to all L8 configurations are consolidated in a single table, including the numerically predicted static strength values, the experimentally measured static yield torque values, and the associated production cost data derived from the defined manufacturing factors. This integrated presentation enables a direct and systematic comparison of strength and cost-related performance metrics, providing a comprehensive basis for evaluating the influence of the selected geometric parameters on the static strength behavior and manufacturability of involute spline connections.

Table 5. Summary of analytical, experimental, and production cost results for the Taguchi L8 orthogonal array.

Experiment Number	A(Width)	B (Root Type)	C (Diametral pitch (DP) & tooth count)	Experimental Static Yield Torque (Nm)	NIEMANN /WINTER	Cost Index (€)
1	10 mm	Flat Root Side Fit	16/32" DP 8T 30° PA	229.7	183	130
2	10 mm	Flat Root Side Fit	32/64" DP 16T 30° PA	215.4	169.6	155
3	10 mm	Fillet Root Side Fit	16/32" DP 8T 30° PA	204.5	219.6	150
4	10 mm	Fillet Root Side Fit	32/64" DP 16T 30° PA	212.3	213.8	175
5	20 mm	Flat Root Side Fit	16/32" DP 8T 30° PA	227.9	303.2	155
6	20 mm	Flat Root Side Fit	32/64" DP 16T 30° PA	223.8	278	180
7	20 mm	Fillet Root Side Fit	16/32" DP 8T 30° PA	209.3	366.2	175
8	20 mm	Fillet Root Side Fit	32/64" DP 16T 30° PA	233.5	352.5	200

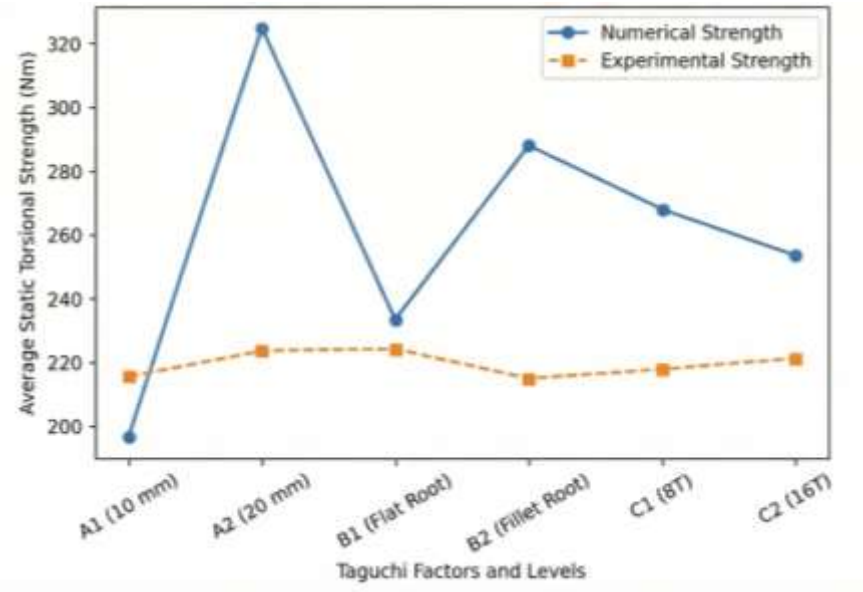

Figure 11. Combined Taguchi Main Effects Plot.

The analytical static strength results obtained using the Niemann/Winter approach provide valuable insight into the influence of the investigated geometric parameters on the load-carrying behavior of involute spline connections. When the numerical results are evaluated factor by factor, contact surface width (Factor A) is identified as the most influential parameter. Increasing the contact width leads to a significant increase in the predicted static strength, which can be attributed to the larger effective contact area and improved load distribution along the spline teeth. This behavior is fully consistent with the fundamental assumptions of the

analytical model, where contact stress and tooth load-sharing govern the strength prediction (Niemann & Winter, 2003).

With respect to spline root geometry (Factor B), the analytical results indicate higher static strength values for fillet root configurations compared to flat root designs. This outcome reflects the reduced stress concentration at the tooth root associated with a larger fillet radius, which is explicitly accounted for in the analytical formulation. From a purely analytical perspective, fillet root splines are therefore expected to exhibit superior static performance due to their improved root stress characteristics.

The influence of diametral pitch and tooth count (Factor C) is also captured in the analytical results, with configurations featuring a lower number of teeth generally showing higher predicted static strength. This trend is explained by increased individual tooth thickness and higher local stiffness, which reduce contact stress levels under static loading conditions. Overall, the analytical evaluation successfully captures the relative effects of the investigated geometric parameters within the framework of tooth contact and tooth root strength criteria.

In contrast to the analytical predictions, the experimental static torsion tests revealed a different governing failure behavior. For all tested spline configurations, failure consistently occurred in the form of torsional fracture of the spline cross-section, rather than through tooth contact damage or tooth root failure. Post-test examinations confirmed that the spline teeth remained largely intact, with no pronounced signs of tooth shear or root cracking prior to fracture. This observation indicates that, under the applied monotonic torsional loading conditions, the load-carrying capacity of the spline connection was governed by the torsional strength of the spline shaft cross-section rather than by the tooth-level strength mechanisms emphasized in the analytical model. As a result, the experimentally measured static yield torque values exhibit smaller variations between different root geometries and tooth configurations than those predicted by the analytical approach. In particular, the expected advantage of fillet root designs observed in the numerical results is not fully reflected in the experimental data, as the failure mechanism is dominated by global torsional stress rather than local tooth root stress. This discrepancy highlights a fundamental limitation of static spline strength evaluations based solely on tooth contact and root stress criteria when cross-sectional torsion becomes the controlling factor (Budynas & Nisbett, 2020).

4. CONCLUSION

This study experimentally and analytically investigated the static strength of involut spline connections. The experimental results demonstrated that failure of the investigated involute spline connections consistently occurred through torsional fracture of the spline cross-section rather than tooth contact or tooth root damage. This finding indicates that static strength evaluations based solely on tooth-level stress criteria may be insufficient when cross-sectional torsion governs the failure mechanism. Consequently, both tooth strength and spline cross-sectional torsional strength should be considered in engineering design to achieve reliable and safe spline connections.

ACKNOWLEDGEMENTS

This work was financially supported by **TAAC Aerospace**. The authors also gratefully acknowledge **TAAC Aerospace** for providing access to the analytical software tools and for supporting the manufacturing of the test specimens used in this study.

REFERENCES

[1] American Gear Manufacturers Association. (2016). Rating of involute spline connections (AGMA 6123-C16).

[2] American Gear Manufacturers Association. (2018). Design considerations for involute splines—General engineering information (AGMA 945-A18).

[3] American National Standards Institute. (2011). Involute splines and inspection criteria (ANSI B92.1-1996 [R2011]).

[4] Budynas, R. G., & Nisbett, J. K. (2020). Shigley's mechanical engineering design (11th ed.). McGraw-Hill Education.

[5] Deutsches Institut für Normung. (2011). DIN 5480: Involute splines based on reference diameters. DIN.

[6] Gupta, P., & Kundu, S. (2019). Investigation on involute spline coupling under misalignment using finite element analysis. Journal of Mechanical Design, 141(7), 071401. https://doi.org/10.1115/1.4043775

[7] Kumar, A., & Singh, R. (2021). Performance analysis of crowned involute splines using finite element analysis. International Journal of Precision Engineering and Manufacturing, 22(3), 545–553. https://doi.org/10.1007/s12541-021-00476-9

[8] Michałowski, J., & Gaska, D. (2018). Effect of spline geometry modification on load distribution and contact stress. Mechanism and Machine Theory, 126, 230–241. https://doi.org/10.1016/j.mechmachtheory.2018.05.009

[9] Niemann, G., & Winter, H. (2003). Machine elements (Vol. II). Springer.

[10] Ross, P. J. (1996). Taguchi techniques for quality engineering. McGraw-Hill.

[11] Taguchi, G. (1986). Introduction to quality engineering. Asian Productivity Organization.

[12] Yadav, S., & Pathak, H. (2020). Multi-response optimization of spline couplings using Taguchi and grey relational analysis. Procedia Manufacturing, 48, 1140–1148. https://doi.org/10.1016/j.promfg.2020.05.156